

## Tuning the properties of silica aerogels through pH controlled sol-gel processes

Fatoş Koç, Selay Sert Çok, Nilay Gizli

Online Publication Date: 02 March 2020

URL: <http://www.jresm.org/archive/resm2019.166ma1203.html>

DOI: <http://dx.doi.org/10.17515/resm2019.166ma1203>

Journal Abbreviation: *Res. Eng. Struct. Mater.*

### To cite this article

Koc F, Sert Cok S, Gizli N. Tuning the properties of silica aerogels through pH controlled sol-gel processes. *Res. Eng. Struct. Mater.*, 2020; 6(3): 257-269.

### Disclaimer

All the opinions and statements expressed in the papers are on the responsibility of author(s) and are not to be regarded as those of the journal of Research on Engineering Structures and Materials (RESM) organization or related parties. The publishers make no warranty, explicit or implied, or make any representation with respect to the contents of any article will be complete or accurate or up to date. The accuracy of any instructions, equations, or other information should be independently verified. The publisher and related parties shall not be liable for any loss, actions, claims, proceedings, demand or costs or damages whatsoever or howsoever caused arising directly or indirectly in connection with use of the information given in the journal or related means.



Published articles are freely available to users under the terms of Creative Commons Attribution - NonCommercial 4.0 International Public License, as currently displayed at [here](https://creativecommons.org/licenses/by-nc/4.0/) (the "CC BY - NC").



Research Article

## Tuning the properties of silica aerogels through pH controlled sol-gel processes

Fatoş Koç<sup>a</sup>, Selay Sert Çok<sup>b</sup>, Nilay Gizli<sup>c</sup>

Department of Chemical Engineering, Ege University, Turkey

### Article Info

### Abstract

#### Article history:

Received 03 Dec 2019

Revised 15 Feb 2020

Accepted 25 Feb 2020

#### Keywords:

Silica aerogel;

Sol-gel reactions;

pH effect;

Monolithic structure

In this study, silica aerogels were produced by two-step sol-gel method to investigate the effect of pH on the physical, chemical and textural structure of aerogels. Tetraethyl orthosilicate (TEOS) used as a silica source. (3-aminopropyl) triethoxysilane (APTES) acted as a silica co-precursor. The quantity of sol precursors kept constant through the experiments and the pH of hydrolysis and condensation reactions were varied. As a result of the experimental studies, the optimum pH values to achieve monolithic aerogel were obtained when the pH of hydrolysis is 3 and the pH of condensation is 10. Physical, chemical and morphological characteristics of the samples were examined by performing FTIR and SEM and density analyses. Results showed that the sample SG-pH3/7 had also well-defined porous structure with homogenous pore distribution, a stable lightweight and monolithic form.

© 2020 MIM Research Group. All rights reserved.

## 1. Introduction

Silica aerogels are nano-structured materials with high porosity (80% - 95%), high surface area (500-1200 m<sup>2</sup>/g), low thermal conductivity, very low density (0.03-0.5 g/cm<sup>3</sup>) and very low dielectric constant (1-8). Silica aerogels are used mainly as thermal and acoustic insulators, catalyst carrier, adsorbent in separation processes, sensor in electronic industry, carrier material in pharmaceutical and agriculture, or as filler material in composite production (2,8,9).

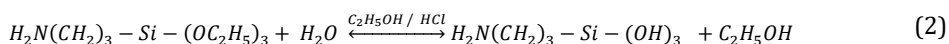
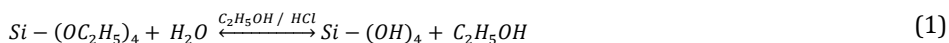
The silica aerogels are mainly synthesized via the traditional sol-gel method. Sol-gel method is generally preferred due to its ease of application in laboratory conditions. Sol-gel reaction is usually based on subsequent hydrolysis and condensation reactions of a sol precursor followed by an aging and a drying period. A general sol-gel process is outlined in Figure 1. This process consists of simultaneous hydrolysis and condensation reactions of a silicon alkoxide group in a liquid solvent with proper acid and/or base catalysis to form a colloidal solution called "sol". Gelation starts because of a condensation reaction, which creates siloxane bridges (Si-O-Si) between Si atoms delivered by precursor molecules that leads to three-dimensional (3D) open network structure. During the gelation, polymeric structure becomes distinct and viscosity of the sol increases (10-13). After complete gelation, the wet gel should be allowed to age over a period of time for the mechanical enhancement of the three-dimensional silica network. At the final step, aged gels are dried by several drying methods to remove the solvents from the pores and to obtain silica aerogels with three-dimensional porous network (14,15). Gel shrinkage, which is one of

\*Corresponding author: [fatoskoc@outlook.com](mailto:fatoskoc@outlook.com)

<sup>a</sup> [orcid.org/0000-0002-2996-110X](https://orcid.org/0000-0002-2996-110X); <sup>b</sup> [orcid.org/0000-0001-7595-2151](https://orcid.org/0000-0001-7595-2151); <sup>c</sup> [orcid.org/0000-0002-7591-1365](https://orcid.org/0000-0002-7591-1365);  
DOI: <http://dx.doi.org/10.17515/resm2019.166ma1203>

the major drawbacks in obtaining monolithic silica aerogel, generally causes from organic solvent evaporation during the aging period. It can be avoided by replacing organic solvent with some other solvent that has a lower vapor pressure. Ionic liquids are organic salts with an extremely low vapor pressure over a large temperature range (-96 to 400 °C), hence, they do not evaporate during long aging periods (19). For that reason, including ionic liquids in the sol-gel reactions may yield a stable gel network and can preserve the structure against gel shrinkage. On the other hand, adding an amine containing silica source can be a good approach in satisfying the silica network in the process. Yang et al. prepared a silica aerogel by following a two-step method in which a silica co-precursor containing an amine group 3-aminopropyltriethoxysilane (APTES) was involved to the sol. They reported that amine-rich APTES behaved like both a basic catalyst and additional silica source and enhance the solid network (16).

Hydrolysis reactions can take place as follows:



Condensation reaction took place as follows:

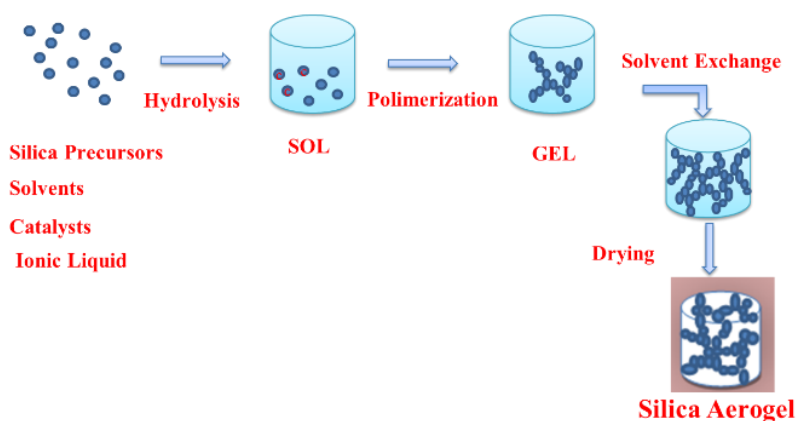
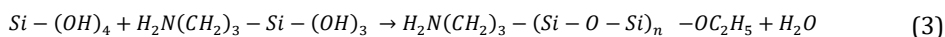


Fig. 1 Schematic presentation of sol-gel process.

The silica aerogels can be produced in various forms (i.e. powders, granular, or monolithic) according to specific target and altering the final form of these materials is possible only by changing the synthesis conditions. Producing silica aerogels in monolithic form has some advantages for particular applications as it allows controlling final shape of the product and has some superior physical properties (i.e. lower thermal conductivity) than the other forms. During the sol-gel method, any process parameters such as composition of the sol, reaction temperature, reaction pH, type of catalysts, drying conditions etc. have great importance on the final chemical, physical and morphological properties of the product. Among these parameters, pH value of the solutions in sol-gel reactions are of the essence on the formation of the 3D structural network and the final physical form of the aerogels (17-19). It directly affects the rates of the hydrolysis and

condensations reactions and the rates of these reactions are vital factors in achieving desired properties of aerogels.

During the sol-gel reaction, hydrolysis and condensation reactions take place simultaneously with different rates. When the sol is converted into a gel, the general variation of the hydrolysis and condensation reaction rates according to pH of the solution is shown in Figure 2. As seen from the Figure 2, the selected pH values can change the rates of these reactions and accelerating, or decelerating rate of these reactions completely change the reaction kinetics. The pH is a key parameter to control the microstructure of gels forming from the sol. The rate of hydrolysis and condensation reactions strongly depends on the acidity of the reaction media. Thus, reactions under acidic or basic conditions must be studied separately. The minimum reaction rate for hydrolysis is at pH 7 and for condensation at around pH 4-5. At pH lower than 5, hydrolysis reaction is favored, and condensation is the rate-limiting step. In this pH range, lots of monomers or small oligomers with reactive Si-OH groups are formed simultaneously. On the contrary, hydrolysis reaction becomes the rate-limiting step at pH higher than 5, and hydrolyzed species are instantly formed due to the faster condensation.

When pH range is between 4-7, the reaction rate of condensation is proportional to the concentration of the OH<sup>-</sup> ions. When pH is less than 2, the silicic acid species becomes positively charged and the reaction rate of the condensation is proportional to the concentration of H<sup>+</sup>. Under strongly basic conditions, the solutions mostly include anionic species. Hence, the rate of Si-O-Si breaking or redissolution of particles is high at elevated pH (Figure.2) (11,20).

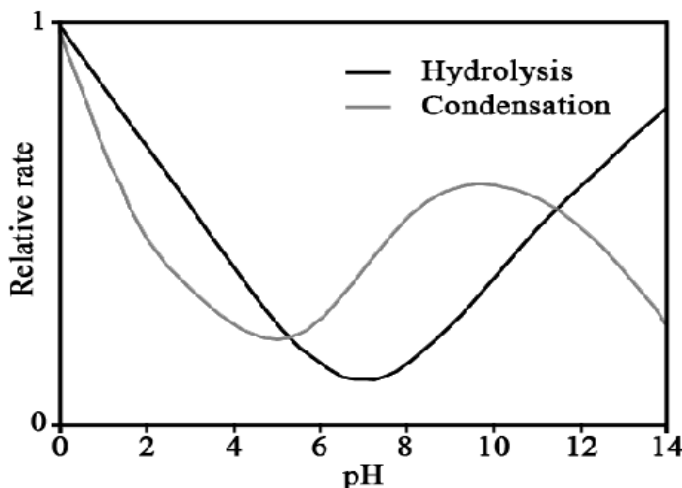


Fig. 2 Hydrolysis and condensation reaction rates depending on pH (21).

In this study, the effect of pH on the final physical and morphological properties of silica aerogels are comprehensively investigated. Achieving monolithic form of silica aerogels after drying period is another crucial target for the study. pH of the solutions was varied either in hydrolysis or condensation reactions as two parts. In the first part of the study, three samples prepared by changing the pH of the solution during hydrolysis reaction as 3, 4 and 5 while keeping the pH of the solution constant during the condensation period. By this way, the proper value of pH for the hydrolysis period was determined in order to

obtain a monolithic crack-free structure. In the second part of the study, pH value in hydrolysis reaction kept constant and the pH of the condensation reaction was varied as 8,9 and 10. Final physical and chemical form of the aerogels were analyzed to determine optimum condensation reaction pH as well. Samples obtained at favorable combination of reaction pHs were then physically, chemically and morphologically characterized.

## 2. Materials and Method

### 2.1. Materials

Silica aerogels were prepared by two-step sol-gel process followed by ambient pressure drying. Tetraethylorthosilicate (TEOS, 98%), 3-aminopropyl-triethoxysilane (APTES) used as silica precursors were purchased from Sigma Aldrich. Ethanol (EtOH) and n-Hexane were used as solvents; HCl, NH<sub>4</sub>OH were involved in sol-gel process as catalyst. 1-ethyl-3-methylimidazolium bis(trifluoromethanesulfonyl)imide (EMIMTF2N) as imidazolium based ionic liquid (IL, 98%) was supplied from Sigma Aldrich and selected as drying control agent to give the final product a crack-free monolithic structure.

### 2.2. Preparation of silica aerogel

The silica aerogels were prepared by following two-step sol-gel process (Figure 3). This process consists of three main parts called as sol preparation and gelation, aging of the gel and drying.

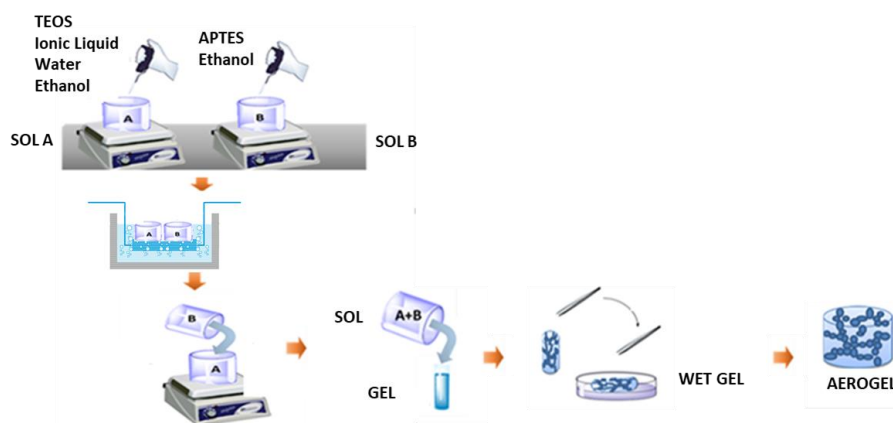


Fig. 3 Two step sol gel method.

During the sol preparation, two silane sources, TEOS and APTES were used. TEOS were hydrolyzed in the presence of IL and EtOH by using 0.01 M HCl for 30 min (sol A) whereas APTES were hydrolyzed only with EtOH for 30 min (sol B). After 30 min of mixing, the solutions were kept in a cold medium to satisfy a proper bonding between particles and hence to enhance the silica network. During the hydrolysis reactions, the silanol polar groups formed by hydrolysis attack each other to form covalent bonds, through simultaneously occurred condensation reaction. Sol A and Sol B are then combined for further continuation of the condensation reaction and fully completion of gelation. pH values of the solution which directly affects the rate of the formation reactions, were adjusted by using HCl. In the first step of this study (run 1), the pH value of hydrolysis in Sol A was adjusted as 3, 4 and 5 in Solution A, while pH of the Sol B was kept constant at 7.

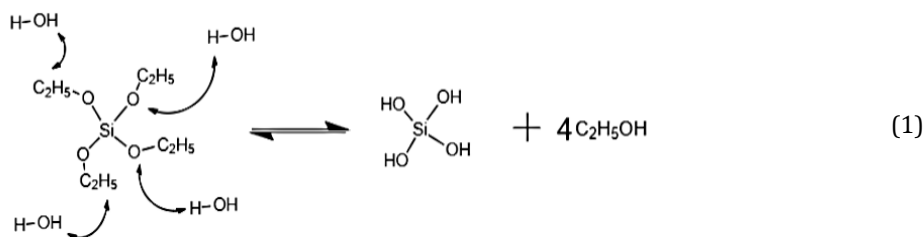
During the condensation period, the solution transformed from liquid state to gel form and ended up with the 3-dimensional network structure. The gelation rate of the sample is directly dependent on the kinetics of the condensation reaction. In the second part of the study (run2), the pH of the condensation reactions was adjusted as 8, 9 and 10 while keeping pH value of the hydrolysis reactions constant. The sol components in all samples and pH values of hydrolysis/condensation periods in run1 and run2 are shown in Table 1.

Table 1. Sol components of all samples in run 1 and run 2.

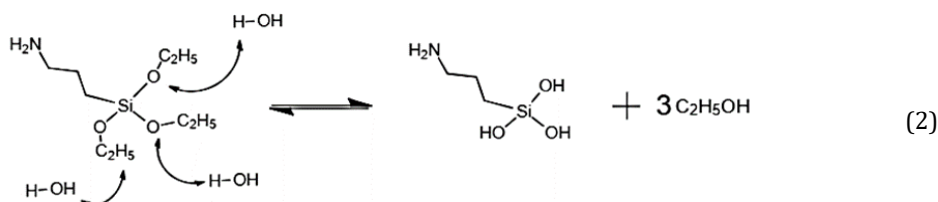
| Run   | ID          | Molar ratios of sol components<br>(mol/mol TEOS) | pH of Hydrolysis period | pH of Condensation period |
|-------|-------------|--|-------------------------|---------------------------|
|       |             | TEOS: APTES: IL: Water: EtOH                     |                         |                           |
| Run 1 | SG- pH 3/7  | 1: 0.141: 0.016: 5.167: 35.67                    | 3                       | 7                         |
|       | SG- pH 4/7  | 1: 0.141: 0.016: 5.167: 35.67                    | 4                       | 7                         |
|       | SG- pH 5/7  | 1: 0.141: 0.016: 5.167: 35.67                    | 5                       | 7                         |
| Run 2 | SG- pH 3/8  | 1: 0.141: 0.016: 5.167: 35.67                    | 3                       | 8                         |
|       | SG- pH 3/9  | 1: 0.141: 0.016: 5.167: 35.67                    | 3                       | 9                         |
|       | SG- pH 3/10 | 1: 0.141: 0.016: 5.167: 35.67                    | 3                       | 10                        |

Hydrolysis and condensation reactions of silica precursors take place as follows:

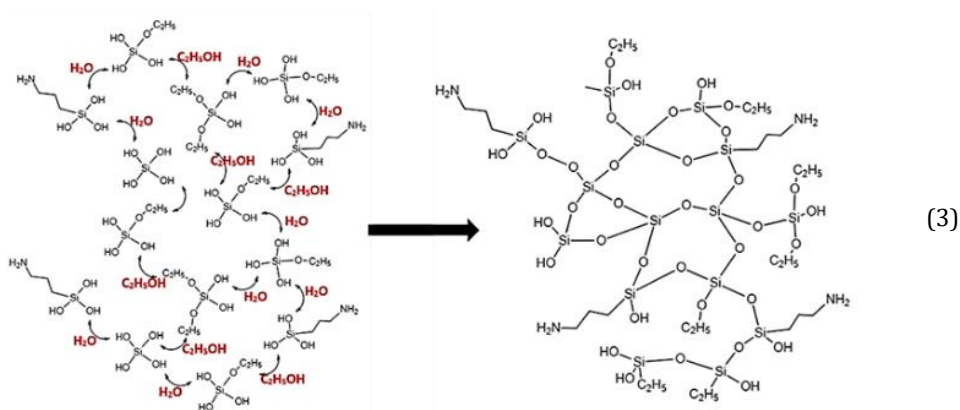
Hydrolysis reaction of TEOS:



Hydrolysis reaction of APTES:



Condensation reaction and the formation 3D structure:



After achieving complete gelation, the silica aerogels were exposed to an aging period of 24 h in a polypropylene cylindrical mold to allow further continuation of the condensation reactions. Afterward, silica aerogels were subjected to ambient pressure drying for 48 hours.

### 2.3 Characterizations

Bulk densities of dried gels were determined by using pycnometer. The percentages of porosity of the samples were estimated according to equation given below (Eq. 1);

$$\% \text{Porosity} = \left(1 - \frac{\rho}{2.1}\right) \times 100 \tag{1}$$

Where  $\rho$  is the bulk density of synthesized silica aerogel and  $2.1 \text{ g/cm}^3$  is the density of solid skeleton (10).

The morphological characterizations of the prepared silica aerogels were evaluated by using Scanning Electron Microscope (SEM) (PHILIPS, XL 30S FEG) with a magnification rate of 10000. Fourier Transform Infrared Spectroscopy (FTIR) (PERKIN ELMER, Spectrum 100, ABD) analysis was performed between the wave number ranges of  $500$  to  $4000 \text{ cm}^{-1}$  to identify the chemical interactions within the samples.

Surface area, average pore volume and average pore diameters of silica aerogels were measured by physisorption of  $\text{N}_2$  at  $77 \text{ K}$  by using Quantachrome Corporation, Autosorb6. Before the measurement, the samples were subjected to degassing operation at  $120^\circ\text{C}$  over night to remove residual moisture and adsorbed gases.

## 3. Results and Discussion

### 3.1 Physical Characterization of Aerogels

Visual observations and the density of the resulted material became our preliminary criteria to decide the optimum pH for hydrolysis. In the first part, three gels were hydrolyzed under the different media having various pH. The monolithic structure was only achieved with the one which has the hydrolysis pH of 3. When the pH of hydrolysis is increased to 4 or 5, samples are obtained in powder form as seen in Figure 4.

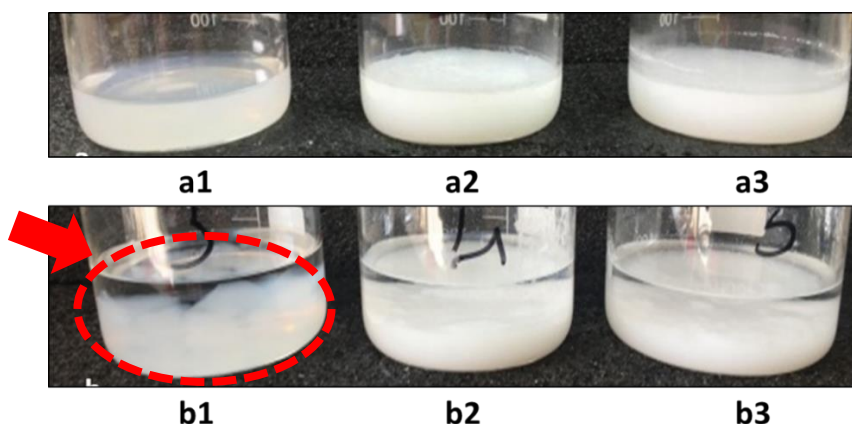


Fig. 4 Visual observations of prepared aerogels a1) SG-pH3/7, a2) SG-pH4/7, a3) SG-pH5/7 at gelation steps and b1) SG-pH3/7, b2) SG-pH4/7, b3) SG-pH5/7 at solvent extraction step.

In the hydrolysis mechanisms, a nucleophilic attack of oxygen ion pairs of the  $H_2O$  molecule on the Si atoms occurs firstly. Due to the polarized Si–O bonds, the silicon atoms carry a partially positive electronic charge, which in that case determines the kinetics of the nucleophilic attack and thus determines the overall hydrolysis reaction. In alkoxides, the Si atoms hold a partially moderate positive charge. Hence, the gelation kinetics of  $Si(OC_2H_5)_4$  alkoxides get so slow unless the hydrolysis and condensation steps of Si are catalyzed either by bases that hold strong negative charges or by acids in which case the reaction mechanism changes drastically (11,21).

In the sol-gel reactions, the relative magnitudes of the hydrolysis and condensation rates are slow enough to allow an almost independent control. In general, silica gels with a texture closer to that of long silica chains in polymeric structures obtained if the hydrolysis rate becomes faster than the condensation rate. This was the case under acidic conditions in our study (SG-pH3/7). Therefore, more stable silica gel network was constructed at the pH value of 3. On the other hand, when the pH of the hydrolysis and condensation reaction are getting closer as in the case of sample SG-pH4/7 and sample SG-pH5/7, reactions can not be dominated by other reaction and it leads shorter silica chain length. Remained alkoxy groups due to the incomplete hydrolysis reaction hinder silica molecules from formation well defined  $SiO_2$  structure. For these reasons, the second part of the study was conducted by adjusting the pH of the hydrolysis reaction 3 and the pH of the condensation reactions was varied from 8 to 10 by addition of 0.1 M base catalysts ( $NH_4OH$ ). The same procedure was followed during synthesis and after drying in ambient condition, only one sample (SG-pH3/10) exhibited a high degree of monolithicity. At this pH in condensation reactions (pH=10) proton acceptors, i.e., bases accelerated the condensation reactions higher than hydrolysis reaction, which then promotes the formation of denser silica colloids (SG-pH3/10).



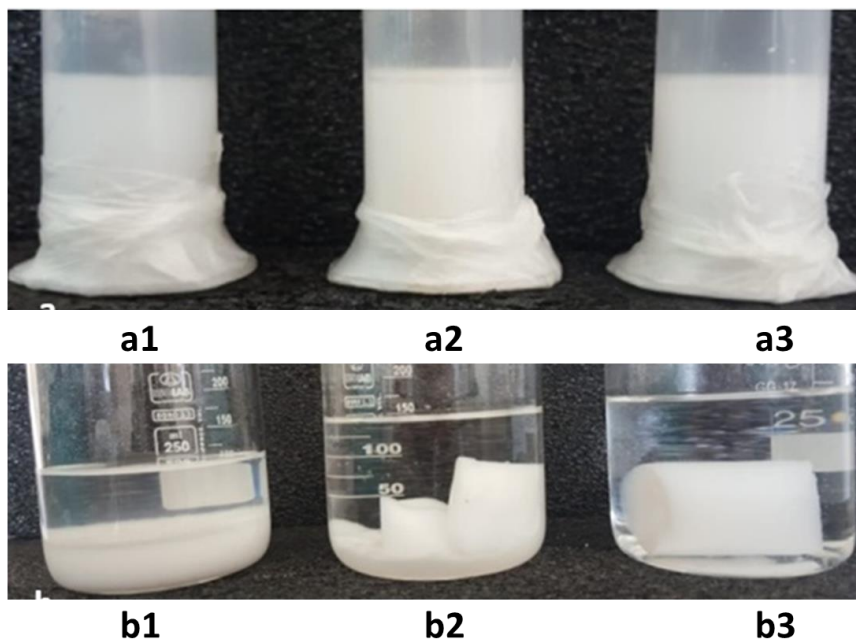


Fig. 5 Visual observations of prepared aerogels a1) SG-pH3/8, a2) SG-pH3/9, a3) SG-pH3/10 at gelation steps and b1) SG-pH3/8, b2) SG-pH3/9, b3) SG-pH3/10 at solvent extraction step.

The density and porosity for the samples are shown in Table 2.

Table 2. Physical properties of the all samples.

| Run   | ID          | Density (g/cm <sup>3</sup> ) | Porosity (%) | Physical observations |
|-------|-------------|------------------------------|--------------|-----------------------|
| Run 1 | SG- pH 3/7  | 0.32                         | 73.3         | monolithic            |
|       | SG- pH 4/7  | 0.29                         | 75.8         | powder                |
|       | SG- pH 5/7  | 0.27                         | 77.5         | powder                |
| Run 2 | SG- pH 3/8  | 0.31                         | 74.1         | Powder                |
|       | SG- pH 3/9  | 0.24                         | 80.0         | granular              |
|       | SG- pH 3/10 | 0.35                         | 70.8         | monolithic            |

The density of each sample was measured by pycnometer and the percentage porosity were determined. A slight increase in the porosity observed with the increase in the pH in hydrolysis reactions. One possible reason for this situation can be the reduction in the superiority of the two reactions to each other owing to the adjustment of the pH at a moderate value. On the other hand, it would not be right to state this comment for the second part. The pH adjusted during the condensation period did not directly affect the porosity of the samples. When the pH of condensation reaction is increased up to 9 the porosity of the samples increased accordingly. On the other hand, when the pH of the condensation reaction adjusted at 10, reaction rate reached the maximal point and as the hydrolysis rate at this pH approached almost to the condensation rate, the porous structure deteriorated at this pH. The density value of the sample SG-pH3/10 was measured as 0.35 g/cm<sup>3</sup> and the porosity value was determined as 70.8 percent. The final

sample had a slightly denser structure than the other samples, probably resulted from the monolithic form of the aerogel.

### 3.2 Chemical Characterization

FTIR analysis was performed to determine chemical structures of aerogels and the FTIR spectrums was given in Figure 6 and 7.

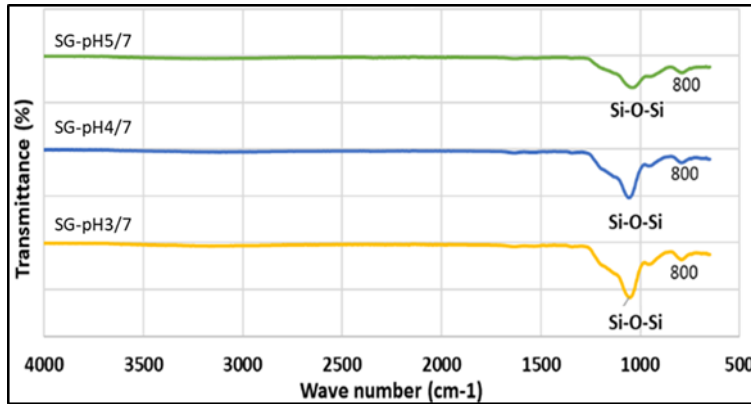


Fig. 6 FTIR spectrum of the prepared aerogels at the pH of 3, 4 and 5.

The values corresponding to peaks near  $1080\text{ cm}^{-1}$  can be attributed to Si-O-Si bonding in the chemical structure of aerogels and indicates the how well the silica network is established (2). As shown in Figure 6, the depth of Si-O-Si bonds at  $1081\text{ cm}^{-1}$  decreased as pH increased. Thus, the strongest Si-O-Si bond was obtained at a pH of 3. This indicates that the perfect hydrolysis was achieved at the pH value of 3.

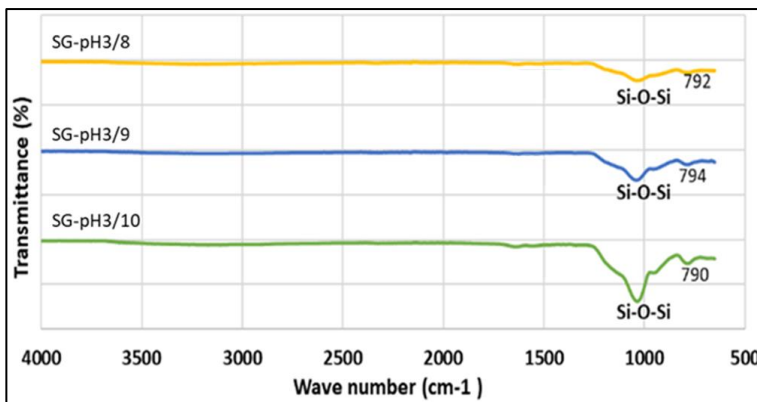


Fig. 7 FTIR spectrum of prepared aerogels at the pH of 8, 9 and 10.

Figure 7 represents the FTIR results of silica aerogels in which the condensation reactions occurs at the pH of 8, 9 and 10. Results have shown that as the pH increased, the condensation reaction accelerated and the intensity of the Si-O-Si bonding increased.

### 3.3 Gelation Behavior

Figure 8 shows the duration of the gelation during the preparation of the samples.

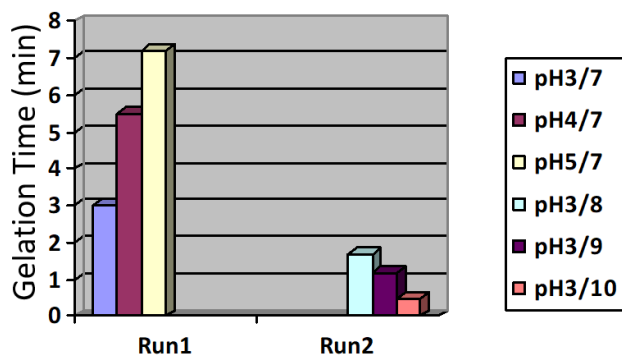


Fig. 8 Gelation time of run1 and run2.

It was observed that when the pH of the condensation reaction is about 7, it took relatively longer time to achieve complete gelation. However, the gelation times at pH higher than 7 occurs fast, which means that there was hardly any time for the system to condensate into a well-defined network. In such gelation times, the generation of larger pores also inevitable. These larger pores act as scattering centers for light in the visible range of the spectrum and caused opacity of the final aerogel, too. As shown in Figure 9, the sample SG-pH 3/10, which showed rapid gelation, had a more opac appearance than the SG-pH 3/7 that has slow gelation.



Fig. 9 Visual observation of the samples SG-pH3/7 and SG-pH3/10, respectively.

### 3.4 Morphological characterization

Microstructural patterns of the produced silica aerogels (SG-pH3/7, SG-pH4/7, SG-pH5/7 and SG-pH3/10) were examined via SEM analysis.

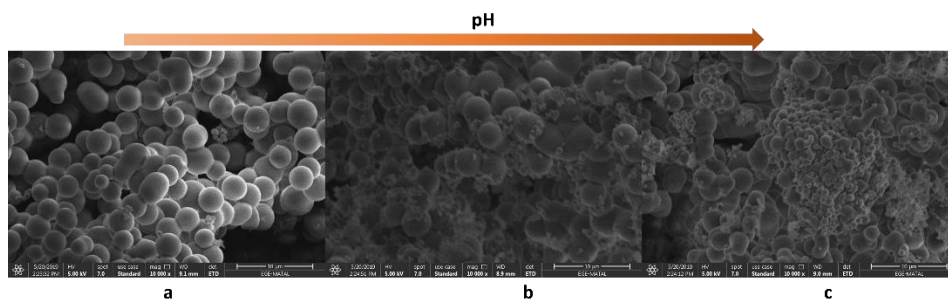


Fig. 10 SEM Image (x10000) of the samples a)SG-pH3/7, b)SG-pH4/7, c)SG-pH5/7.

SEM images confirmed the results about the existence of well-defined primary silica particles in SG-pH3/7 rather than other samples in run1. Due to completion of sufficient hydrolysis during the synthesis of the sample SG-pH3/7, there observed a homogenously distribution of the nearly same sized silica particles for this sample. When the pH in hydrolysis reaction increased, it yielded less homogenous pore network and non-uniform particle size as in Figure 10b and 10c.

On the other hand, when the condensation reaction increased to 10, regarding to severe Si-O formation and very fast condensation reaction, very small silica particles formed and agglomerated on each other as small clusters as in Figure 11. As a result, SG-pH3/10 yielded less porous form with denser solid structure comparing to SG-pH3/7.

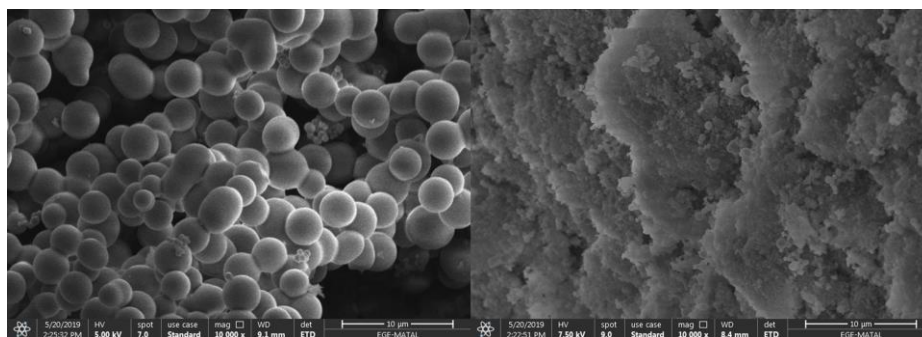


Fig. 11 SEM Image with 10000-magnification rate of the samples SG-pH3/7 and SG-pH3/10, respectively.

Surface area, pore volume and average pore diameter values after Nitrogen adsorption/desorption measurements were summarized in Table 3. BET surface area for SG-pH3/7 exhibited relatively high surface area ( $65 \text{ m}^2/\text{g}$ ) than the SG-pH3/10. Accordingly, average pore volume value also higher for this sample. This outcome is compatible with homogenous distribution of the pores in this sample compared to that of SG-pH3/10. Results also confirm the existence of micropores in the structure for SG-pH3/7, too. Pore dimensions increased as the pH of the condensation reaction increase and for SG-pH3/10 scale of the pores was increased from micro to meso scale.

Table 3. Pore characteristics of silica aerogels

| Sample ID | Specific Surface Area (m <sup>2</sup> /g) | Pore Volume (cm <sup>3</sup> /g) | Average pore diameter (nm) |
|-----------|---|----------------------------------|----------------------------|
| SG-pH3/7  | 65  | 0.147                            | 1.73                       |
| SG-pH3/10 | 37  | 0.050                            | 2.13                       |

#### 4. Conclusions

In this study, the effect of pH that is one of the most crucial parameter affecting the final properties and physical appearances of silica aerogels was investigated. For this purpose, various pH values are examined during the sol-gel reactions. In the first part of the study, three samples prepared by changing the pH of the solution during hydrolysis reaction while keeping the pH of the solution constant during the condensation period. In this way, the appropriate pH was determined as 3 for the hydrolysis period in order to obtain a monolithic crack-free structure (the sample SG-pH3/7). In the second part, pH was varied during the condensation period while keeping pH value constant as three with respect to the previous part. In this part, only one sample (SG-pH3/10) exhibited a high degree of monolithicity. At this pH value, the condensation reaction was accelerated more than the hydrolysis step, which then favors the formation of 3D colloidal silica particles and monolithic form of gels (SG-pH3/10).

It was visually observed that only two samples (SG-pH3/7 and SG-pH3/10) have preserved their monolithic structure after drying during this whole study. Although the chemical characteristics defined by FTIR analysis were similar, density measurements exhibited that the sample SG-pH3/7 had slightly lighter and more porous than the sample SG-pH3/10. At the same time, SEM and BET analyses have identified that the sample SG-pH3/7 had a well-defined and homogenous size of primary particles with higher specific surface area and pore volume.

#### References

- [1]Laskowski J, Milow B, Ratke L. Aerogel-aerogel composites for normal temperature range thermal insulations. *J Non Cryst Solids*, 2016;441:42-8. <https://doi.org/10.1016/j.jnoncrsol.2016.03.020>
- [2]Soleimani Dorcheh A, Abbasi MH. Silica aerogel; synthesis, properties and characterization. *J Mater Process Technol.* 2008;199(1):10-26. <https://doi.org/10.1016/j.jmatprotec.2007.10.060>
- [3]Maleki H, Durães L, Portugal A. An overview on silica aerogels synthesis and different mechanical reinforcing strategies. *J Non Cryst Solids*, 2014;385:55-74. <https://doi.org/10.1016/j.jnoncrsol.2013.10.017>
- [4]Pons A, Casas L, Estop E, Molins E, Harris KDM, Xu M. A new route to aerogels: Monolithic silica cryogels. *J Non Cryst Solids*. 2012;358(3):461-9. <https://doi.org/10.1016/j.jnoncrsol.2011.10.031>
- [5]Amonette JE, Maty J. Microporous and Mesoporous Materials Functionalized silica aerogels for gas-phase purification, sensing, and catalysis: A review. 2017;250. <https://doi.org/10.1016/j.micromeso.2017.04.055>
- [6]Maleki H, Durães L, García-gonzález CA, Mahmoudi M. Synthesis and biomedical applications of aerogels: Possibilities and challenges. 2016;236:1-27. <https://doi.org/10.1016/j.cis.2016.05.011>

- [7]Buratti C, Merli F, Moretti E. Aerogel-based materials for building applications: Influence of granule size on thermal and acoustic performance. *Energy Build.* 2017;152:472-82. <https://doi.org/10.1016/j.enbuild.2017.07.071>
- [8]Li Z, Cheng X, He S, Shi X, Gong L, Zhang H. Aramid fibers reinforced silica aerogel composites with low thermal conductivity and improved mechanical performance. *Compos Part A Appl Sci Manuf.*, 2016;84:316-25. <https://doi.org/10.1016/j.compositesa.2016.02.014>
- [9]Li M, Jiang H, Xu D, Hai O, Zheng W. Low density and hydrophobic silica aerogels dried under ambient pressure using a new co-precursor method. *J Non Cryst Solids*, 2016;452:187-93. <https://doi.org/10.1016/j.jnoncrysol.2016.09.001>
- [10]Wei TY, Chang TF, Lu SY, Chang YC. Preparation of monolithic silica aerogel of low thermal conductivity by ambient pressure drying. *J Am Ceram Soc.* 2007;90(7):2003-7. <https://doi.org/10.1111/j.1551-2916.2007.01671.x>
- [11]Shi F, Wang L, Liu J. Synthesis and characterization of silica aerogels by a novel fast ambient pressure drying process. *Mater Lett.* 2006;60(29-30):3718-22. <https://doi.org/10.1016/j.matlet.2006.03.095>
- [12]Hilonga A, Kim JK, Sarawade PB, Kim HT. Low-density TEOS-based silica aerogels prepared at ambient pressure using isopropanol as the preparative solvent. *J Alloys Compd.* 2009;487(1-2):744-50. <https://doi.org/10.1016/j.jallcom.2009.08.055>
- [13]Vioux A, Viau L, Volland S, Le Bideau J. Use of ionic liquids in sol-gel; ionogels and applications. *Comptes Rendus Chim.* 2010;13(1-2):242-55. <https://doi.org/10.1016/j.crci.2009.07.002>
- [14]Wu C, Lin S. Preparation and Fractal-Structure Characterization of Monolithic Silica Aerogel with a Short-Chain Ionic Liquid as the Solvent. 2010;126:123-6. <https://doi.org/10.14723/tmrjs.37.123>
- [15]Smitha S, Shajesh P, Aravind PR, Kumar SR, Pillai PK, Warriar KKG. Effect of aging time and concentration of aging solution on the porosity characteristics of subcritically dried silica aerogels. *Microporous Mesoporous Mater.* 2006;91(1-3):286-92. <https://doi.org/10.1016/j.micromeso.2005.11.051>
- [16]Dourbash A, Motahari S, Omranpour H. Effect of water content on properties of one-step catalyzed silica aerogels via ambient pressure drying. *J Non Cryst Solids*, 2014;405:135-40. <https://doi.org/10.1016/j.jnoncrysol.2014.09.013>
- [17]Sinkó K. Influence of chemical conditions on the nanoporous structure of silicate aerogels. *Materials (Basel)*. 2010;3(1):704-40. <https://doi.org/10.3390/ma3010704>
- [18]Schubert U. Sol - Gel Chemistry and Methods. *Sol-Gel Handb Synth Charact Appl.* 2015;1-28. <https://doi.org/10.1002/9783527670819.ch01>
- [19]Wu CM, Lin SY, Chen HL. Structure of a monolithic silica aerogel prepared from a short-chain ionic liquid. *Microporous Mesoporous Mater.*, 2012;156:189-95. <https://doi.org/10.1016/j.micromeso.2012.02.039>
- [20]Juan Vivero. *Silica Nanoparticles; preparation, properties and uses.* Vol. 1, Nova Science Publisher, Inc. 2012. 53 p.
- [21]Bera S, Udayabhanu G, Narayan R, Rout TK. *Sol-Gel Process for Anti-Corrosion Coatings.* 2013;209-31.
- [22]Sachithanadam M, Chandrakant Joshi S. *Silica Aerogel Composites.* Engineering Materials. 2016. <https://doi.org/10.1007/978-981-10-0440-7>